**UDC 550.340**

Andriy GNYP, Dmytro MALYTSKYY

Carpathian Branch of Subbotin Institute of Geophysics, National Academy of Sciences of Ukraine, 3B, Naukova str., Lviv, 79060, Ukraine, e-mail: agnyp.gm@gmail.com, https://orcid.org/0000-0002-2612-4234

https://doi.org/10.23939/jgd2025.02.171

# RECOVERING LOCATIONS AND TAKEOFF ANGLES OF EARTHQUAKES IN CLUSTERS BASED ON THE DIFFERENCE IN THEIR S-P INTERVALS

It is demonstrated in [Gnyp & Malytskyy, 2023] that only the difference in the intervals between the first P- and S-waves can be used to relocate a cluster of similar earthquakes. The advantage of using only the difference is that it is measured by cross-correlation within a window containing the corresponding arrivals, eliminating the need to know their exact timing. Another advantage is that relative locations can be recovered regardless of source times and, therefore, of often inaccurate arrival picks or velocity models. It is assumed in [Gnyp & Malytskyy, 2023] that the cluster size is significantly smaller than the distance to the stations, and that the takeoff angles of the first P- and S-waves, as well as station azimuths, are known for at least one reference earthquake. Under these conditions, the relationship between the locations and the difference becomes purely geometrical and linear, allowing for a straightforward solution of the corresponding system. However, if both the locations and takeoff angles are unknown, the system becomes nonlinear and singular, making it nearly impossible to solve. In the current version of the algorithm, we propose circumventing the singularity by optimizing the locations and takeoff angles separately. First, we determine the locations for some initial angles, then adjust the angles, re-evaluate the locations, and repeat this process. To evaluate the effectiveness of this approach, we conduct a series of synthetic experiments, focusing primarily on the ability to achieve complete recovery of locations and takeoff angles using a damped least-squares solution, depending on the accuracy of the initial angles, the number and configuration of stations, and the damping applied. To reduce the impact of local minima, we propose estimating the median of solutions obtained for an ensemble of randomly perturbed initial angles. The tests demonstrate the effectiveness of the algorithm and its potential applicability to real data. The algorithm can be combined with other relocation techniques, which makes it possible to link the poorly recorded events to well-constrained ones. This is particularly important for clearer imaging of fault structures in intraplate areas with low seismicity, improving our understanding of local seismic activity and earthquake hazard.

*Keywords:* earthquake location, takeoff angles, relocation, similar earthquakes, cluster earthquakes, S-P interval, cross-correlation.

## Introduction

The similarity of earthquakes occurring in clusters is now widely used to measure their relative (differential) phases, thereby significantly improving their location accuracy, both relative and absolute [Shearer, 1997; Menke, 1999; Waldhauser & Ellsworth, 2000; Shearer et al., 2005; Snieder & Vrijlandt, 2005; Robinson et al., 2007, 2007, 2013]. Consequently, a large number of small earthquakes can be included in the analysis [Papadimitriou et al., 2023; Bonatis et al., 2024], which is crucial to many problems of seismological research, especially in regions with low local seismicity, such as the East Carpathians [Gnyp, 2010, 2013, 2021, 2022; Kozlovskyi et al., 2020; Nazarevych et al., 2022].

In our previous study [Gnyp & Malytskyy, 2023], we proposed an algorithm for relocating earthquakes that occur in clusters, based on the simultaneous comparison of a large number of intervals between their first S- and P-waves. One advantage of using only the difference is that, since it is measured by cross-correlation within a *window* around the corresponding phases, there is no need to know exact arrival times. Another advantage is that, since only *relative* locations are recovered, this can be done regardless of source times and, therefore, of often inaccurate phase picks or velocity models.

In [Gnyp & Malytskyy, 2023], we assume that, since the cluster size is much smaller than the distance to the stations, (i) the ray paths are nearly identical outside the cluster, and differences in travel times arise only within the cluster; (ii) changes in station azimuths and takeoff angles due to location changes are very small and can be neglected. It is also assumed that (iii) the rays lie in a vertical plane containing both the earthquake and the station; (iv) the P- and S-wave velocities ($v_P$ and $v_S$) are known and uniform within the cluster; (v) the azimuths of the stations also are known for at least one, reference earthquake, as well as the takeoff angles of the first P- and S-waves. Under these assumptions, the relationship between the difference in intervals and the coordinates of earthquakes within a local Cartesian system centered on the reference earthquake becomes purely geometric and linear, making it easy to solve the corresponding system of equations.

 

A series of synthetic experiments was conducted in [Gnyp & Malytskyy, 2023] to evaluate the algorithm's performance. It depended on several factors, including the number and configuration of stations, the level of noise in the observed data, data sparsity, and inaccuracies in azimuths and takeoff angles. In the experiments, differences in the intervals between S- and P-waves were generated for some original locations and subsequently used as observables to recover the locations by solving the corresponding linear system. The tests demonstrate the algorithm's effectiveness and its potential applicability, particularly for small earthquakes or sparse networks where a large portion of the data is noisy or missing.

The assumptions in the initial version of our algorithm, although numerous, are in fact very realistic and common in seismological practice. Usually, the location and takeoff angles for at least the largest earthquake can be determined by other methods, which serve as a reference. Since the cluster size is much smaller than the distance to the stations – a condition that is often met – it is reasonable to assume that the station azimuth and takeoff angles are the same for all earthquakes, and that the ray paths identical outside the cluster. Besides, the rays generally lie within a vertical plane containing both the source and the station, with very rare exceptions due to the extremely inhomogeneous velocity structure.

On the other hand, numerous assumptions significantly limit the algorithm's potential applicability. Theoretically, the station azimuths and takeoff angles can be recovered simultaneously with the locations. However, if the problem is approached directly, the resulting nonlinear system becomes so singular that it is practically unsolvable.

In a new version of our algorithm, we propose circumventing the singularity by optimizing the locations and takeoff angles separately. First, we determine the locations for some initial angles, then adjust the angles, re-evaluate the locations, and repeat this process. At the same time, to simplify the problem – at least at this stage – we assume that the station azimuths are known and that their inaccuracies are much smaller than those of the take-off angles.

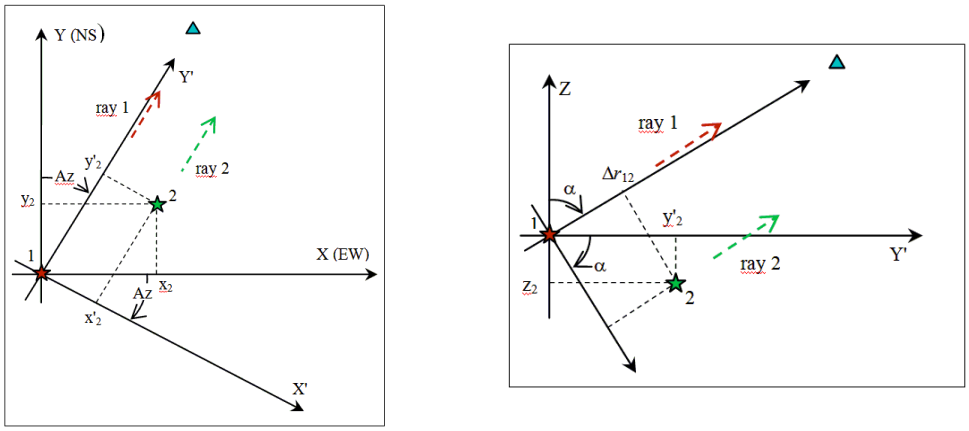


**Fig. 1.** Scheme for calculating the difference between the ray paths from earthquakes 1 and 2 with coordinates $x_1$, $y_1$, $z_1$, and $x_2$, $y_2$, $z_2$ in the local Cartesian system. On the left is the horizontal projection, on the right is the vertical one. Earthquakes are indicated with red and green stars, and the station, which is actually much further away, is indicated with a blue triangle. a is the angle of emergence.

## Algorithm

The difference $DDSP_{ij}^{(k)}$ in the intervals between P- and S-waves for a pair of earthquakes $i$ and $j$ at station $k$ is defined as

$$DDSP_{ij}^{(k)} = t_i^{(k)} + S_i^{(k)} - (t_i^{(k)} + P_i^{(k)}) - (t_j^{(k)} + S_j^{(k)}) + t_j^{(k)} + P_j^{(k)},$$

$$= S_i^{(k)} - S_j^{(k)} - (P_i^{(k)} - P_j^{(k)}), = DS_{ij}^{(k)} - DP_{ij}^{(k)},$$

in which $t_i$ and $t_j$ are the source times, $S_i^{(k)}$, $S_j^{(k)}$, $P_i^{(k)}$, and $P_j^{(k)}$ are the travel times of first P- and S-waves, $DP_{ij}^{(k)}$ and $DS_{ij}^{(k)}$ are the travel time differences between earthquakes $i$ and $j$ measured by the cross-correlation between the corresponding waveforms at station $k$, $i$, $j$ = 1,…, $N$, and $k$ = 1,…, $K$. For $N$ earthquakes, there will be $N(N\text{-}1)$ pairs and the same number (or sometimes fewer) of differences (observations) at each station.

Under the assumptions made in the previous version of our algorithm [Gnyp & Malytskyy, 2023], the dependence of differences on coordinates becomes purely geometric and linear (Fig. 1):

$$DDSP_{ij}^{(k)} = da^{(k)}(x_j - x_i) + db^{(k)}(y_j - y_i) + dc^{(k)}(z_j - z_i), \quad (1)$$

in which

$$da^{(k)} = \sin(-Az^{(k)})\sin(-\beta^{(k)})/v_S - \sin(-Az^{(k)})\sin(-\alpha^{(k)})/v_P,$$

$$db^{(k)} = -\cos(-Az^{(k)})\sin(-\beta^{(k)})/v_S + \cos(-Az^{(k)})\sin(-\alpha^{(k)})/v_P, \quad (2)$$
$$dc^{(k)} = \cos(-\beta^{(k)})/v_S - \cos(\alpha^{(k)})/v_P,$$

the axes X and Y of the local Cartesian system centered on the first earthquake are directed east and north, respectively; the axis Z is directed upwards, $Az^{(k)}$ is the azimuth of the *k*-th station, and $\alpha^{(k)}$ and $\beta^{(k)}$ are the takeoff angles of the P- and S-rays measured clockwise relative to the Z axis.

The equations (1) are linear with respect to the coordinates, and can be easily solved if angles $\alpha^{(k)}$ and $\beta^{(k)}$, and $Az^{(k)}$ are known.

After introducing vectors

$$\mathbf{X} \equiv (x_2, y_2, z_2, x_3, y_3, z_3, \dots, x_N, y_N, z_N)^{\mathrm{T}},$$
$$\text{and } \mathbf{\Delta\Delta SP}^{(k)} \equiv (\Delta\Delta SP_{12}^{(k)}, \Delta\Delta SP_{13}^{(k)}, \dots, \Delta\Delta SP_{1N}^{(k)},$$
$$\Delta\Delta SP_{23}^{(k)}, \Delta\Delta SP_{24}^{(k)}, \dots, \Delta\Delta SP_{2N}^{(k)}, \dots, \Delta\Delta SP_{N-2N-1}^{(k)},$$
$$\Delta\Delta SP_{N-2N}^{(k)}, \Delta\Delta SP_{N-1N}^{(k)})^{\mathrm{T}},$$

equations (1) can be presented in the matrix form:

$$\mathbf{D}^{(k)}\mathbf{X} = \mathbf{\Delta\Delta SP}^{(k)}, \quad (3)$$

in which the matrix $\mathbf{D}^{(k)}$ consists of the expressions (2) for $a^{(k)}$, $b^{(k)}$ and $c^{(k)}$, and its dimensions are $(N\text{-}1)\cdot N/2 \times 3\cdot(N\text{-}1)$. The structure of the system (3) is transcribed in Appendix 1 to [Gnyp & Malytskyy, 2023].

After introducing matrix **D** and vector **ΔΔSP**

$$\mathbf{D} \equiv \begin{bmatrix} \mathbf{D}^{(1)} \\ \mathbf{D}^{(2)} \\ \vdots \\ \mathbf{D}^{(K)} \end{bmatrix}, \quad \mathbf{\Delta\Delta SP} \equiv \begin{bmatrix} \mathbf{\Delta\Delta SP}^{(1)} \\ \mathbf{\Delta\Delta SP}^{(2)} \\ \vdots \\ \mathbf{\Delta\Delta SP}^{(K)} \end{bmatrix},$$

the system of equations for K stations is obtained:

$$\mathbf{DX} = \mathbf{\Delta\Delta SP}, \quad (4)$$

in which the dimensions of matrix **D** are $K\cdot(N\text{-}1)\cdot N/2 \times 3\cdot(N\text{-}1)$.

It is demonstrated in [Gnyp & Malytskyy, 2023] that if accurate takeoff angles are known, locations **X** can be fully recovered by solving equation (4) using the differences from at least three stations in the absence of noise in the data, **ΔΔSP**. Otherwise, if accurate takeoff angles are not known and we start with some assumed ones, there will be no exact solution **X** to (4), because even if there is another set of angles and locations for which the differences **ΔΔSP** are exactly the same, or even if such sets are multiple, it is very unlikely that we would be able to stumble upon them by chance. In the current version of our algorithm, we minimize the least squares norm:

$$L = \left|\mathbf{\Delta\Delta SP} - \mathbf{DX}\right|^2. \quad (5)$$

When both the observations **ΔΔSP** (actually the additive noise **n** in them) and the model **X** are considered multidimensional random processes with components of each of them statistically independent and with the same dispersions, $\sigma_n$ and $\sigma_m$, respectively, the stochastic inversion of [Aki and Richards, 1980] is equivalent to the familiar and frequently used damped least squares:

$$\mathbf{X} = (\mathbf{D}^{\mathrm{T}}\mathbf{D} + \varepsilon^2\mathbf{I})^{-1}\mathbf{D}^{\mathrm{T}}\,\mathbf{\Delta\Delta SP}, \quad (6)$$

in which the damping parameter $\varepsilon^2$ means $\sigma_n$ to $\sigma_m$ ratio. Increasing $\varepsilon^2$ damps the influence of diagonal elements in the $\mathbf{D}^{\mathrm{T}}\mathbf{D}$ that are smaller than $\varepsilon^2$, thereby reducing its singularity and improving the likelihood of obtaining a physically meaningful solution. However, this also decreases its resolution, defined as the number of statistically independent components.

Next, we proceed to the optimizing of takeoff angles.

Since a change in the takeoff angles, $\alpha^{(k)}$ and $\beta^{(k)}$, of the rays traveling to station *k* does not affect the difference in the intervals at other stations, the angles can only be optimized individually for each of the stations. So, for simplicity, we will drop the station's number *k* in the superscript and instead use *O* and *S* to represent the observed and synthetic variations, respectively. Therefore, the least squares optimization of angles can be represented as the minimization of the norm:

$$A = \left|\mathbf{\Delta\Delta SP}^O - \mathbf{\Delta\Delta SP}^S(\alpha,\beta)\right|^2, \quad (7)$$

in which

$$\mathbf{\Delta\Delta SP}^O \equiv (\Delta\Delta SP_{12}^{(k)}, \Delta\Delta SP_{13}^{(k)}, \dots, \Delta\Delta SP_{1N}^{(k)},$$
$$\Delta\Delta SP_{23}^{(k)}, \Delta\Delta SP_{24}^{(k)}, \dots, \Delta\Delta SP_{2N}^{(k)}, \dots, \Delta\Delta SP_{N-2N-1}^{(k)},$$
$$\Delta\Delta SP_{N-2N}^{(k)}, \Delta\Delta SP_{N-1N}^{(k)})^{\mathrm{T}}$$

are the differences observed at station *k*, $k = 1, \dots, K$, and $\mathbf{\Delta\Delta SP}^S$ are the synthetic differences calculated for some takeoff angles, α and β, which are the same for all cluster earthquakes.

After linearization of $\mathbf{\Delta\Delta SP}^S(\alpha,\beta)$ in the vicinity of $\alpha^*$ and $\beta^*$, the norm *A* becomes

$$A = \left|\mathbf{d} - \mathbf{Gm}\right|^2, \quad (8)$$

in which

$$\mathbf{d} = \mathbf{\Delta\Delta SP}^O - \mathbf{\Delta\Delta SP}^S(\alpha,\beta)\Big|_{\alpha=\alpha^*,\beta=\beta^*},$$
$$\mathbf{m} = \begin{bmatrix} \alpha - \alpha^* \\ \beta - \beta^* \end{bmatrix},$$

and matrix **G** consists of the two column vectors

$$\mathbf{G} = \left[\frac{\partial\,\mathbf{\Delta\Delta SP}^S(\alpha,\beta)}{\partial\,\alpha}\Big|_{\alpha=\alpha^*}, \frac{\partial\,\mathbf{\Delta\Delta SP}^S(\alpha,\beta)}{\partial\,\beta}\Big|_{\beta=\beta^*}\right]. \quad (9)$$

Then, the column vectors of partial derivatives in **G** can be represented as

$$\frac{\partial\,\mathbf{\Delta\Delta SP}^S(\alpha,\beta)}{\partial\,\alpha}=\mathbf{AX},\ \frac{\partial\,\mathbf{\Delta\Delta SP}^S(\alpha,\beta)}{\partial\,\beta}=\mathbf{BX},$$

in which $N\cdot(N\text{-}1)/2$ by (×) $3\cdot(N\text{-}1)$ matrices **A** and **B** consist of coefficients

$$da1=\sin(-Az)\cos(-\alpha)/v_P\ ,$$
$$da2=-\cos(-Az)\cos(-\alpha)/v_P,$$
$$da3=-\sin(-\alpha)/v_P,$$

and

$$db1=-\sin(-Az)\cos(-\beta)/v_S\ ,$$
$$db2=\cos(-Az)\cos(-\beta)/v_S,$$
$$db3=\sin(-\beta)/v_S,$$

respectively, and are identical in structure to the matrix **D** in (3), transcribed in Annex 1 to [Gnyp & Malytskyy, 2023].

The global minimum of *A* in (8), which is equal to zero, is reached when

$$\mathbf{d}=\mathbf{G}\,\mathbf{m}. \qquad (10)$$

However, due to the inherent inaccuracy of the model, $\mathbf{\Delta\Delta SP}^S(\alpha,\beta)$, an exact solution to (10) either does not exist or the solutions are multiple. So, we use damped least squares again:

$$\mathbf{m}=(\mathbf{G}^{\mathrm{T}}\mathbf{G}+\gamma^2\mathbf{I})^{-1}\mathbf{G}^{\mathrm{T}}\,\mathbf{d}, \qquad (11)$$

in which the meaning of the damping parameter $\gamma^2$ is the same as of $\varepsilon^2$ in (6).

Thus, after optimizing the takeoff angles for each of the stations using damped least squares, the new locations **X** are calculated for them, and so on, until the minimum criteria are met.

### Synthetic experiments

Next, a series of synthetic experiments is performed, in which the "observed" (actual) difference in the intervals between P- and S-waves is generated for some synthetic earthquakes located in an imaginary rupture plane randomly along two 3D lines intersecting at zero coordinates. To avoid inconsistencies and bring the experiments closer to reality, the actual cluster size, takeoff angles, and station azimuths are used, as in the relocation of the Teresva series in [Gnyp & Malytskyy, 2021]. The coordinates of 18 synthetic earthquakes in the local Cartesian system centered on the reference earthquake are listed in Table 1.

*Table 1*

**Coordinates of synthetic earthquakes in the local Cartesian system.**

| | EW, km | NS, km | Z, km |
|---|---|---|---|
| 1 | 2 | 3 | 4 |
| 1 | 0.00 | 0.00 | 0.00 |
| 2 | 9.00 | 9.00 | 9.00 |

*Continuation of Table 1*

| 1 | 2 | 3 | 4 |
|---|---|---|---|
| 3 | -1.00 | -1.00 | -1.00 |
| 4 | -2.00 | -2.00 | -2.00 |
| 5 | 8.00 | 8.00 | 8.00 |
| 6 | -3.00 | -3.00 | -3.00 |
| 7 | 4.00 | 4.00 | 4.00 |
| 8 | 6.00 | 6.00 | 6.00 |
| 9 | 7.00 | 7.00 | 7.00 |
| 10 | 5.00 | 5.00 | 5.00 |
| 11 | 9.00 | -5.85 | 1.35 |
| 12 | -1.00 | 0.65 | -0.15 |
| 13 | -2.00 | 1.30 | -0.30 |
| 14 | 8.00 | -5.20 | 1.20 |
| 15 | -3.00 | 1.95 | -0.45 |
| 16 | 4.00 | -2.60 | 0.60 |
| 17 | 6.00 | -3.90 | 0.90 |
| 18 | 7.00 | -4.55 | 1.15 |
| 19 | 5.00 | -3.25 | 0.75 |

Table 2 shows the takeoff angles and station azimuths (Fig. 2). Velocity $v_P$ is set to 5 and $v_S$ to 3 km/s inside the cluster.

The efficiency of our inversion scheme is then explored by varying the accuracy of the initial takeoff angles, the number and configuration of stations, and the values of the damping parameters $\varepsilon^2$ and $\gamma^2$.

The inaccuracy of the initial angles is modeled by adding random numbers uniformly distributed in the ranges of ±11 and ±20 degrees to the actual angles (Table 2). Since all gradient-based nonlinear optimizations are susceptible to the presence of local minima, we propose reducing their impact by estimating the median of solutions for an ensemble of initial angles, randomly perturbed in a similar manner in the ranges of ±15 and ±23 degrees, respectively, with maximum perturbation reaching ±16 and ±43 degrees.

*Table 2*

**Station azimuths and takeoff angles of the first P- and S-waves (α, β) used to calculate differences in the "observed" S-to-P intervals. Takeoff angles are measured as it is shown in Fig. 1.**

| | Az, deg | □, deg | □, deg |
|---|---|---|---|
| RAK | 97.00 | 73.58 | 64.76 |
| BM | 199.60 | 78.00 | 67.17 |
| MEZ | 343.30 | 79.60 | 67.97 |
| TRS | 272.60 | 79.60 | 68.07 |
| NSL | 306.20 | 66.37 | 59.55 |
| BUR | 112.70 | 85.22 | 70.03 |
| TES | 126.90 | 96.04 | 92.77 |
| DRG | 208.20 | 120.85 | 120.45 |
| MLR | 148.50 | 142.36 | 117.38 |
| GZR | 193.80 | 117.98 | 117.53 |

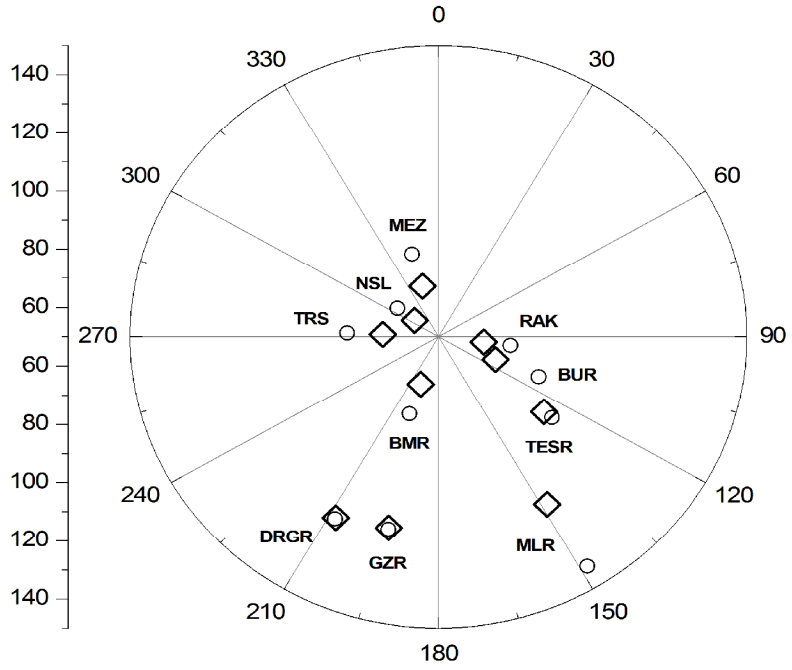


**Fig. 2.** Azimuths of stations and takeoff angles of first P- and S-waves (indicated by circles and diamonds, respectively) (Table 2) used for the calculation of "observed" differences in the intervals between S- and P-waves.

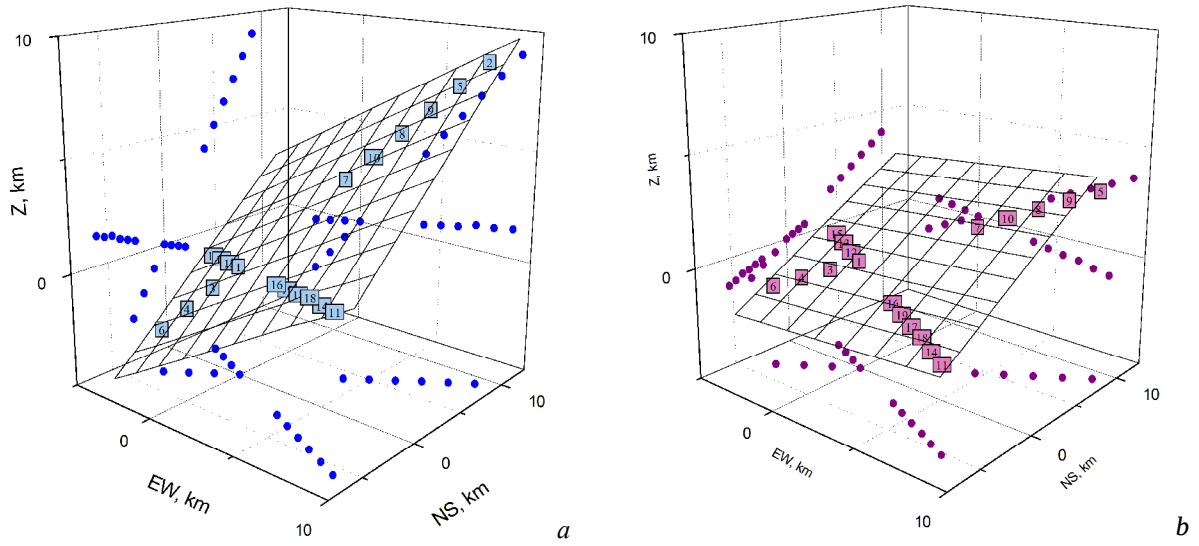


**Fig. 3.** Recovering the locations and takeoff angles of 18 synthetic earthquakes in 3D using five stations: RAK, BMR, MEZ, TRS, and NSL. The inaccuracy of the initial angles is modeled by perturbing the actual angles within the range of ±11 degrees.

*a*: The actual locations of synthetic earthquakes in 3D (Table 1) and the hypothetical rupture plane defined by them. Here and below, the actual locations are indicated by cyan squares, while their projections are depicted as blue circles. The locations are approximated by a surface using the method of correlation grids [Davis, 1986].

*b*: One of ten sets of initial earthquake locations in 3D, calculated for initial angles further perturbed in the ±15-degree range. Here and below, locations are represented by purple squares, and their projections are depicted as purple circles.

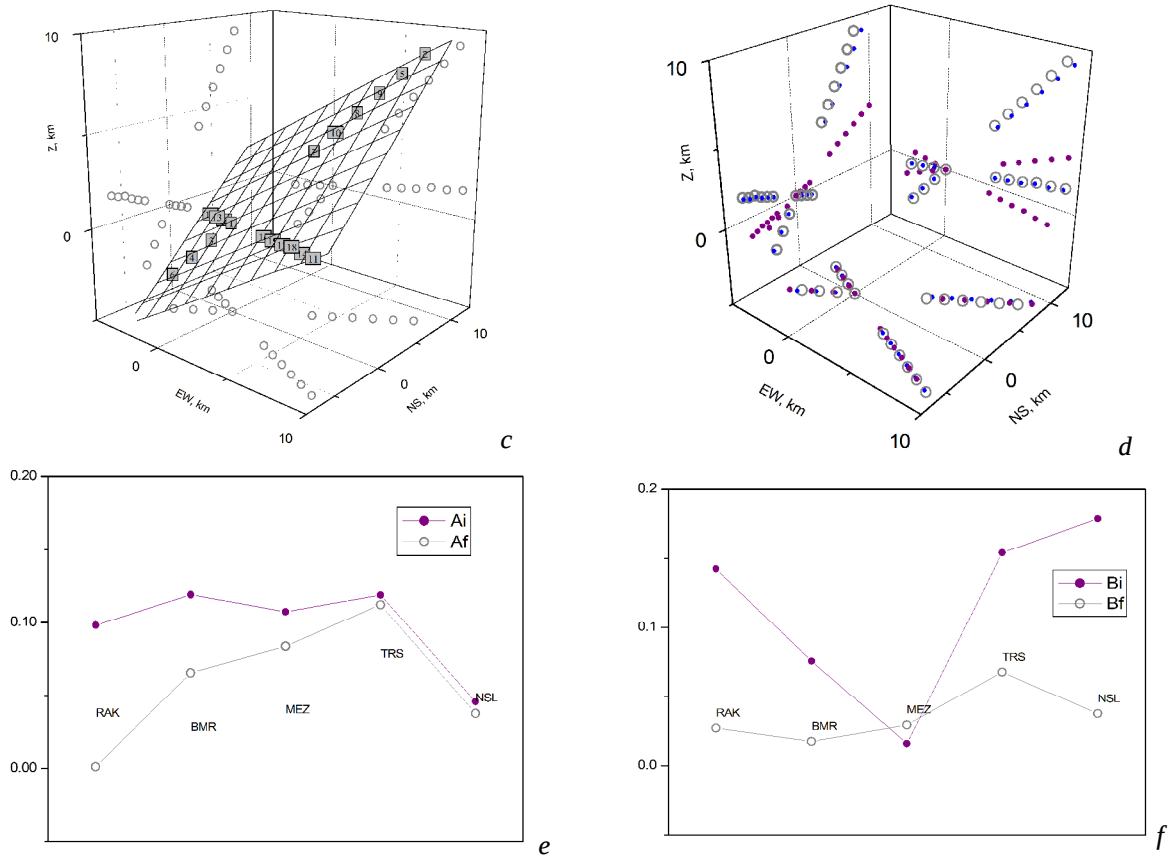


**Fig. 3. (Continuation).** Recovering the locations and takeoff angles of 18 synthetic earthquakes in 3D using five stations: RAK, BMR, MEZ, TRS, and NSL. The inaccuracy of the initial angles is modeled by perturbing the actual angles within the range of ±11 degrees.

*c:* The median of ten sets of final locations. Throughout the article, they are indicated by gray squares, and their projections are denoted by empty circles.

*d:* 2D projections of actual, initial, and median final locations.

*e:* The relative difference between the initial and actual takeoff angles of P-wave (Ai), and between the median final and actual angles (Af).

*f:* The relative difference between the initial and actual takeoff angles of S-wave (Bi), and between the median final and actual angles (Bf).

The recovery of locations is evaluated qualitatively, based on their visual presentation in 3D and 2D (Fig. 3 *a*, *b*, *c*, and *d*). For takeoff angles, relative estimators are used

$$a^i = \left|\alpha^i - \alpha^a\right|/\alpha^a, \quad b^i = \left|\beta^i - \beta^a\right|/\beta^a,$$
$$a^f = \left|\alpha^f - \alpha^a\right|/\alpha^a, \quad b^f = \left|\beta^f - \beta^a\right|/\beta^a,$$

in which superscript $i$ is for the initial angles, $a$ – for the actual angles, and $f$ – for the final (or recovered) ones. The efficiency of the recovery was then judged by the difference between $a^i$ and $a^f$, and $b^i$ and $b^f$, respectively (Fig. 3 *e*, *f*).

Finding the optimal values of damping parameters $\varepsilon^2$ and $\gamma^2$ (6, 11) may be considered a problem in itself. Large values can lead to very small changes in model parameters, significantly slowing down the algorithm's convergence, as well as increasing the risk of ending up in a local minimum. If they are too large, the convergence may not be achieved at all, or the solution may turn out to be meaningless. We select values of $\gamma^2$ and $\varepsilon^2$ experimentally, by trial and error, taking into account the above considerations. For a fixed number of synthetic earthquakes, the optimal values vary depending on the number and configuration of stations, as well as the inaccuracy of the initial angles. As expected, the optimal values for $\gamma^2$ and $\varepsilon^2$ differ by several orders of magnitude, which only reflects the singularity of the problem and a sharp contrast between the metrics of the two model parameter spaces and the metric of the data space [Harris & Douglas, 2021; Málek et al. 2007].

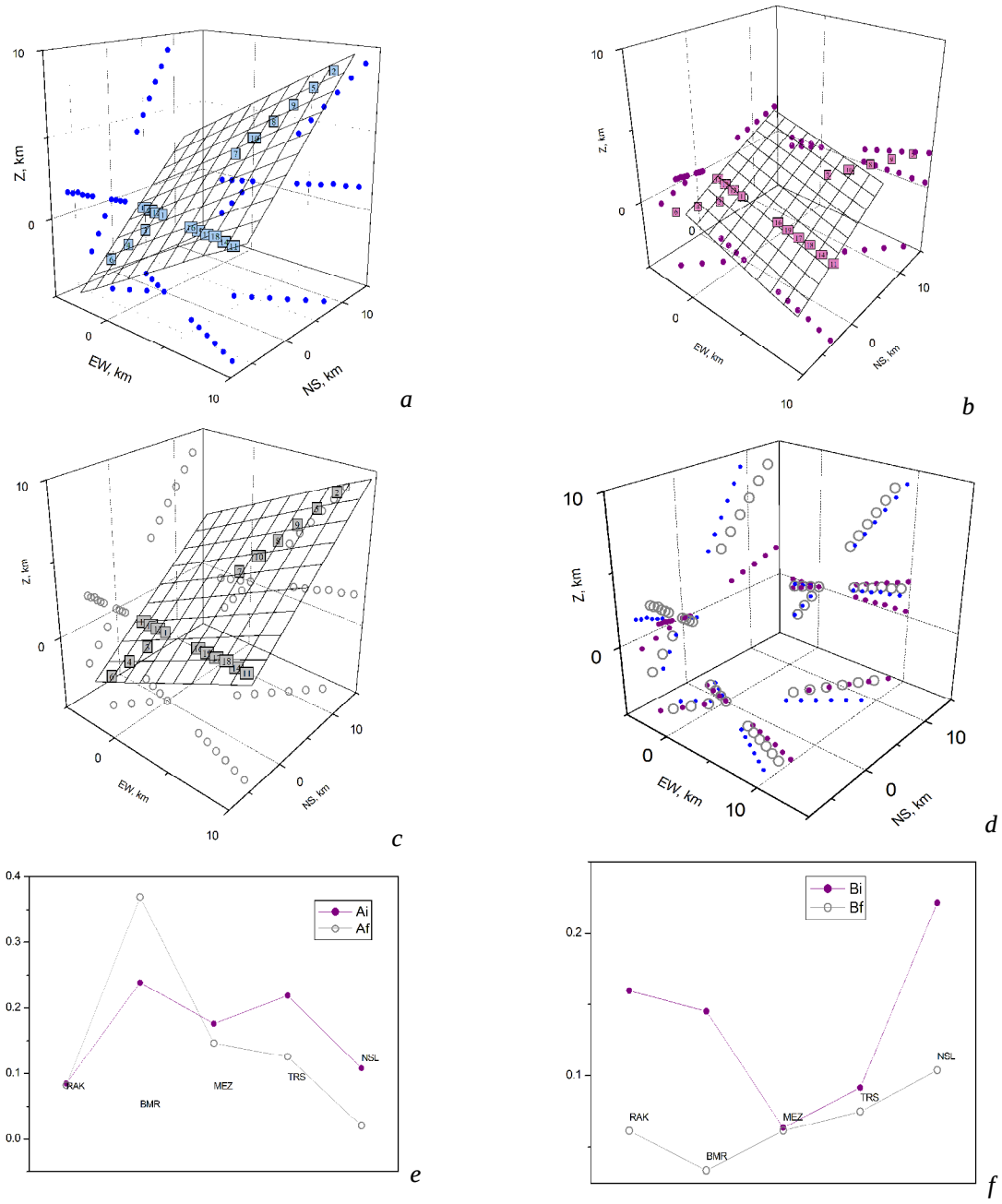


**Fig. 4.** Recovering the locations and takeoff angles of 18 synthetic earthquakes in 3D using five stations: RAK, BMR, MEZ, TRS, and NSL. The inaccuracy of the initial angles is modeled by perturbing the actual angles within the range of ±20 degrees.

*a:* The actual locations of synthetic earthquakes in 3D (Table 1).

*b:* One of ten sets of initial earthquake locations in 3D, calculated for initial angles further perturbed in the ±23-degree range.

*c:* The median of ten sets of final locations.

*d:* 2D projections of actual, initial, and median final locations.

*e:* The relative difference between the initial and actual takeoff angles of the P-wave (Ai), and between the median final and actual angles (Af).

*f:* The relative difference between the initial and actual takeoff angles of S-wave (Bi), and between the median final and actual angles (Bf).

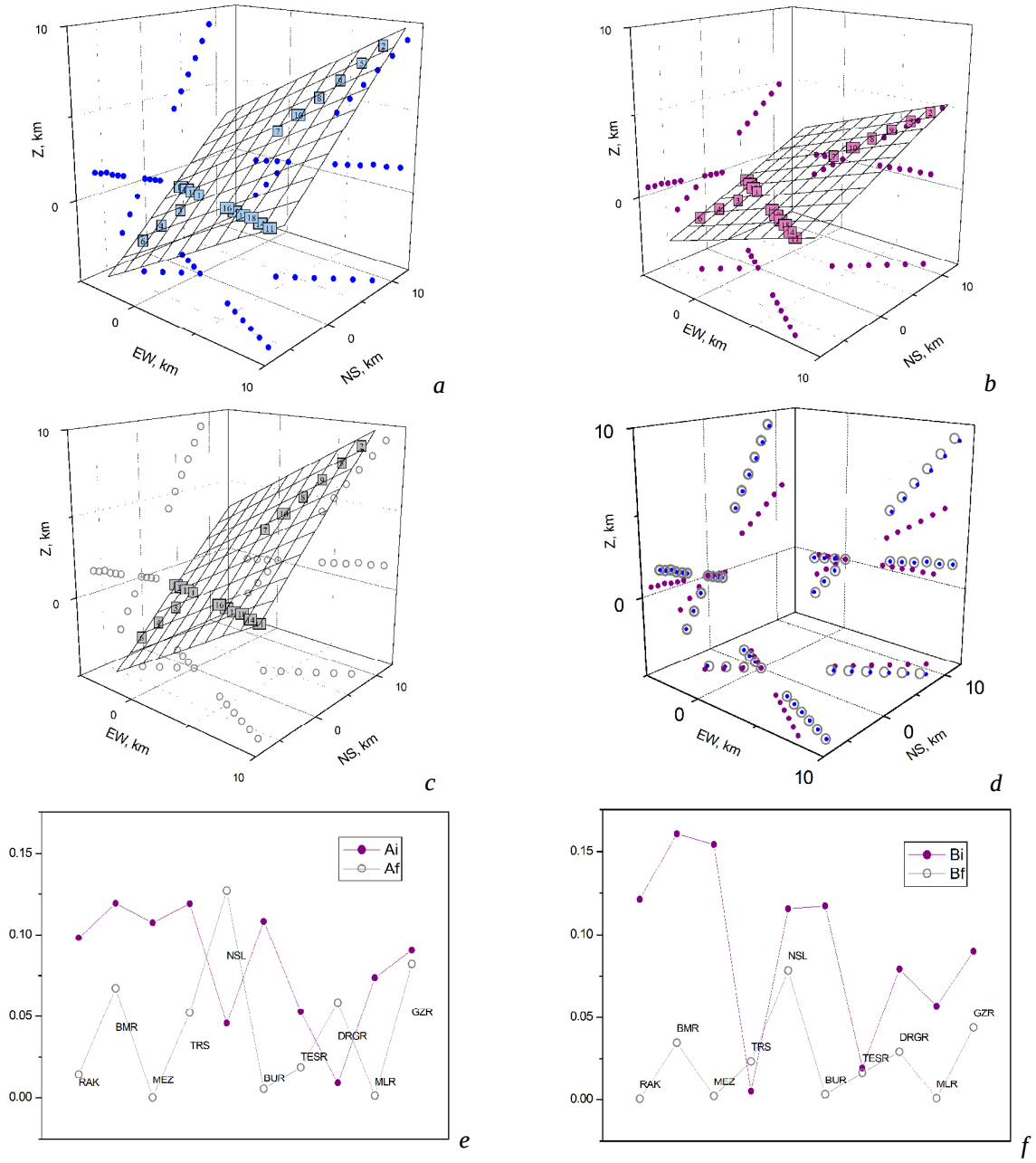


**Fig. 5.** Recovering the locations and takeoff angles of 18 synthetic earthquakes in 3D using all ten stations listed in Table 1. The inaccuracy of the initial angles is modeled by perturbing the actual angles within the range of ±11 degrees.

a: The actual locations of synthetic earthquakes in 3D (Table 1) and the hypothetical rupture plane defined by them.

*b:* One of five sets of initial earthquake locations in 3D, calculated for initial angles further perturbed in the ±15-degree range.

*c:* The median of five sets of final locations.

*d:* 2D projections of actual, perturbed, and median final locations.

*e:* The relative difference between the initial and actual takeoff angles of the P-wave (Ai), and between the median final and actual angles (Af).

*f:* The relative difference between the initial and actual takeoff angles of S-wave (Bi), and between the median final and actual angles (Bf).

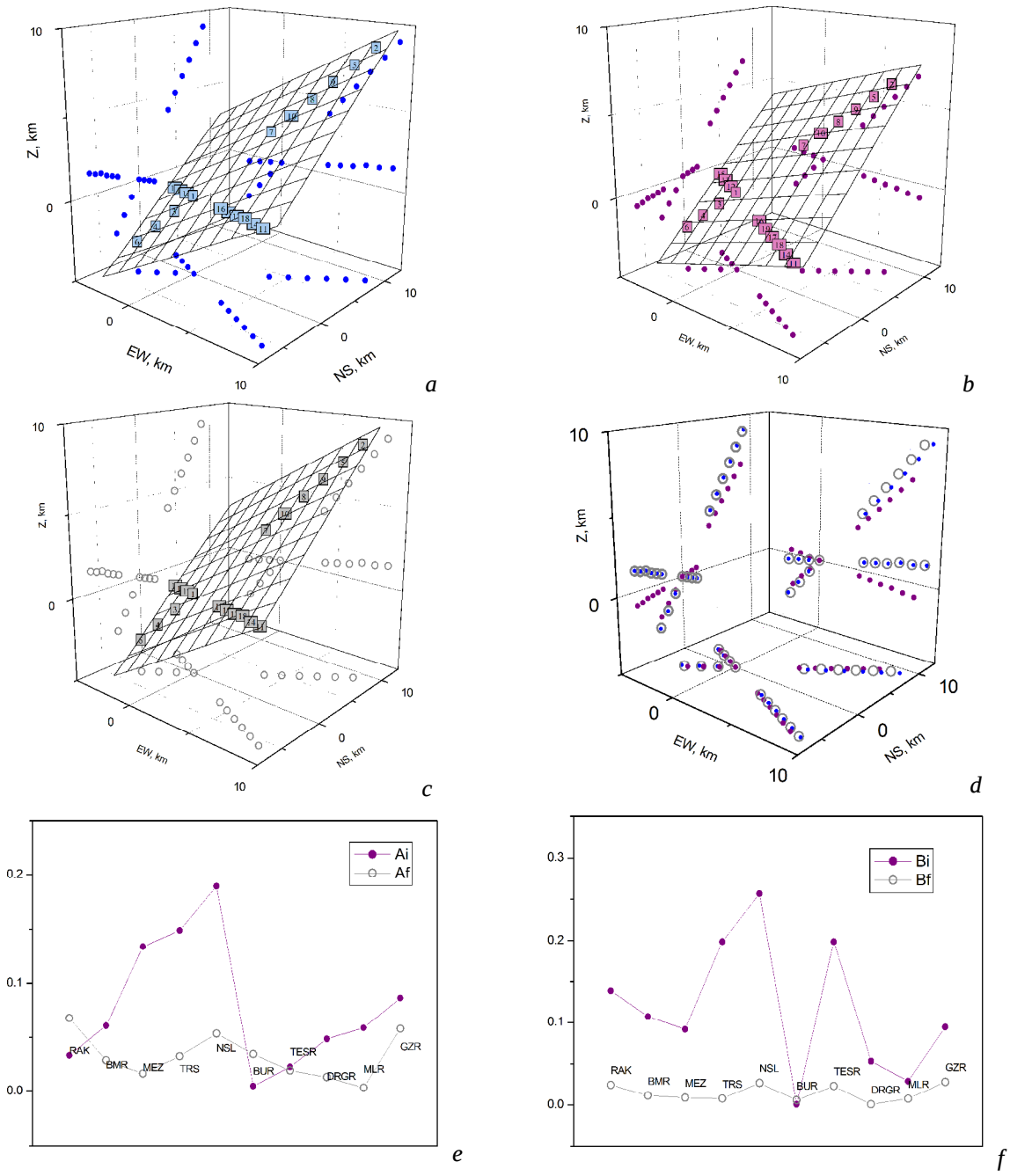


**Fig. 6.** Recovering the locations and takeoff angles of 18 synthetic earthquakes in 3D using all ten stations listed in Table 1. The inaccuracy of the initial angles is modeled by perturbing the actual angles within the range of ±20 degrees.

*a:* The actual locations of synthetic earthquakes in 3D (Table 1).

*b:* One of five sets of initial earthquake locations in 3D, calculated for initial angles further perturbed in the ±23-degree range.

*c:* The median of five sets of final locations.

*d:* 2D projections of actual, perturbed, and median final locations.

*e:* The relative difference between the initial and actual takeoff angles of the P-wave (Ai), and between the median final and actual angles (Af).

*f:* The relative difference between the initial and actual takeoff angles of S-wave (Bi), and between the median final and actual angles (Bf).

Figs. 3 and 4 show the results for 5 stations (RAK, BMR, MEZ, TRS, and NSL), the smallest number of stations for which the solution is uniquely constrained. In Figs. 5 and 6, the results are shown for all ten stations listed in Table 2.

Even with such a large inaccuracy of the initial takeoff angles as ±20 degrees, the improvement in the median of the final locations, not only compared to the initial, but also to the actual locations, is evident in all experiments and can be considered quite satisfactory.

Significant improvements are observed in the median of final takeoff angles, although with some exceptions. It is important to note in this regard that the median of the final solutions is estimated here not from solutions that satisfy the norms $L$ and $A$ (5, 7), but from solutions corresponding to local minima, in which the gradients (9) become close to zero, approaching the smallest representable computer number, and do not change any further. The median in the example with ten stations is estimated using solutions for five perturbed initial takeoff angles, whereas in the example with five stations, ten perturbed initial angles are used. It is quite possible that the median of the final solutions can be further improved simply by increasing their number; however, this requires significantly greater computational power and time.

We present experiments with five and ten stations; the results for six and eight also confirm a steady improvement in recovering both locations and takeoff angles as the number of stations increases.

## Discussion and conclusion

The paper presents a new algorithm for recovering earthquake locations and takeoff angles. It is based on the simultaneous comparison of intervals between S- and P-waves from closely spaced events, such as earthquakes in clusters. The difference between the intervals is measured only by cross-correlation, which means it is not influenced by arrival times. The algorithm can be used even without a velocity model, as long as the location of the reference earthquake is known with reasonable accuracy.

The algorithm can be combined with other relocation techniques, which makes it possible to link the poorly recorded events to well-constrained ones. This is particularly important for achieving clearer imaging of fault structures and understanding of local seismic activity and earthquake hazard in intraplate areas with low seismicity. On the other hand, if the algorithm is applied independently, the link between events can still be established, and the performance of the algorithm can be significantly improved by using a larger number of reference earthquakes.

It is also important to note that, although only the relative locations of earthquakes are recovered, the spatial orientation and size of the cluster are true. If the earthquakes share the same rupture plane, their focal mechanism is the same as the mechanism of the reference earthquake. Thus, the reliability of the mechanism, as determined using an often inaccurate velocity model, can be verified by the recovered orientation of the rupture plane. Furthermore, the takeoff angles, which are also recovered independently of the velocity model, can also be used to verify both the mechanism and the recovered orientation of the rupture plane.

Various other versions of the algorithm can also be proposed. In particular, station azimuths can be recovered. As a result, the horizontal location of the reference earthquake can be verified using the recovered azimuths. On the other hand, it is possible to propose simplified versions of the algorithm in which some parameters are considered to be more or less accurately known, and only the remaining parameters are recovered. Such as the first version of the algorithm, in which the takeoff angles are known. Or, for example, one could consider the option of recovering velocities $v_P$ and $v_S$ within the cluster, while the other parameters are known. Even variations in velocities over time can be implemented in such a version. Thus, a wide range of seismological problems can be addressed using the different versions of the algorithm.

## References


Aki, K., and P.G. Richards (1980). *Quantitative Seismology. Theory and Methods*. Vols. 1 and 2, Freeman and Co., San Francisco, 932 p.

Bonatis, P., Karakostas, V., Papadimitriou, E., & Kourouklas C. (2024). The 2022 $M_w$5.5 earthquake off-shore Kefalonia Island – relocated aftershocks, statistical analysis and seismotectonic implications. *J. Seismol.* https://doi.org/10.1007/s10950-024-10255-y

Davis, J. C. (1986). Statistics and Data Analysis in Geology. *John Wiley & Sons, Inc., Second edition*. https://doi.org/10.23939/jgd2023.02.019

Gnyp, A. (2010). Refining locations of the 2005-2006 recurrent earthquakes in Mukacheve, West Ukraine, and implications for their source mechanism and the local tectonics. *Acta Geophysica*, 58 (4), 587–603. https://doi.org/10.2478/s11600-010-0006-9

Gnyp, A. (2013). Recovering Relative Locations of the 2005-2006 Mukacheve Earthquakes from Similarity of their Waveforms at a Single Station. *Acta Geophysica*, 61 (5), 1074–1087. https://doi.org/10. 24 78/s11600-012-0096-7

Gnyp, A., & Malytskyy, D., (2021). Differential and source terms locations of the 2015 Teresva (East Carpathians) series and their tectonic implications. *Acta Geophysica*, 69 (6), 2099–2112. https://doi.org/10.1007/s11600-021-00655-w https://rdcu.be/cyPNh

Gnyp, A. (2022). Determination of differential locations and focal mechanism of the 2013-2015 earthquakes in Trosnyk, Transcarpatians: methodological aspects and analysis of the results. *Geodynamics,* 2(33), 50–63. https://doi.org/10.23939/jgd2022.02.050

Gnyp A., Malytskyy D. (2023). Relocating earthquakes in clusters based on variations in the intervals between their first *P*- and S-waves, *Geodynamics,* 2(35), 19–32. https://doi.org/10. 23939/jgd2023.02.019

Harris, D. B., & Douglas, A. D. (2021). The geometry of signal space: a case study of direct mapping between seismic signals and event distribution. *Geophys. J. Int.* 224, 2189–2208. https://doi. org/10.1093/gji/ggaa572 https://doi.org/10.3997/2214-4609.201701868.

Kozlovskyi, E, Maksymchuk., V., Malytskyy, D., Tymoschuk, V., Hrytsai, O., & Pyrizhok, N. (2020). Structural-tectonic and seismic characteristics relationships in the Central part of the Transcarpathian internal depression. *Geodynamics,* 1(28), 62–70. https://doi.org/10.23939/ jgd2020.01.062.

Málek, J., Růžek, B., & Kolář, P. (2007). Isometric method: Efficient tool for solving non-linear inverse problems. *Studia Geophysica et Geodaetica,* 51, 469–491. https://doi.org/10.1007/s11200-007-0028-1

Menke, W. (1999). Using waveform similarity to constrain earthquake locations, *Bull. Seismol. Soc. Am.* 89, 4, 1143–1146. https://doi.org/10.1785/0120130004

Nazarevych, A., Nazarevych, L., Bayrak, G., & Pyrizhok, N. (2022). Seismotectonics of the Oash and Transcarpathian deep faults junction zone (Ukrainian Transcarpathians). *Geodynamics,* 2(33), 99–114. https://doi.org/10.23939/jgd2022.02.100

Papadimitriou, E., Karakostas, V., Papazachos, C., Foumelis, M., Kiratzi, A., Pikridas, C., Bonatis, P., Kostoglou, A., Kourouklas, C., Scordilis, E., Bitharis, S., Paradisopoulou, P., Panou, A., Galanis, O., Karagianni, E., Vamvakaris, D., Karagianni, I., Kkallas, C., Chatzis, N., Chatzipetros, A., Fotiou, A., Ventouzi, C., Grendas, I., Kementzetzidou, D., Karakaisis, G., & Hatzidimitriou, P. (2023). The seismogenic structure of March 2021 Tyrnavos (central Greece) doublet ($M_w$ 6.3 and $M_w$ 6.0), constrained by aftershock locations and geodetic data. *Geophys. J. Int*, 235, 644– 689. https://doi.org/10.1093/gji/ggad253

Robinson, D. J, Sambridge, M., & Sneider, R. (2007), Constraints on coda wave interferometry estimates of source separation: The acoustic case. *Explor. Geophys*. 38(3), 189–199. https://doi.org/10.1071/EG07019

Robinson, D. J, Sneider, R., & Sambridge, M. (2007) Using coda wave interferometry for estimating the variation in source mechanism between double couple events. *J. Geophys. Res,* 112(B12), B12302. https://doi.org/10.1029/2007JB004925

Robinson, D. J, Sambridge, M., Sneider, R., & Hauser, J. (2013). Relocating a Cluster of Earthquakes Using a Single Seismic Station. *Bull. Seism. Soc. Am,* 103(6), 3057–3072. https://doi.org/10.1785/0120130004

Shearer, P. M. (1997), Improving local earthquake locations using L1 norm and waveform cross-correlation: Application to the Whittier Narrows, California, aftershock sequence. *J. Geophys. Res.* 102(B4), 8269–8283. https://doi.org/10.1029/96JB03228

Shearer, P., Hauksson, E., & Lin, G. (2005). Southern California hypocenter relocation with waveform cross-correlation. Part 2: Results using source-specific station terms and cluster analysis. *Bull. Seism. Soc. Am*, 95(3), 904–915. https://doi.org/10.1785/01200401168

Snieder, R., & Vrijlandt, M. (2005). Constraining the source separation with coda wave interferometry: Theory and application to earthquake doublets in the Hayward Fault, California, *Journal of Geophysical Research: Solid Earth*, 110(B4), https://doi.org/10.1029/2004JB003317

Waldhauser, F, & Ellsworth, L.W. (2000). A Double-Difference Earthquake Location Algorithm: Method and Application to the Northern Hayward Fault. California. *Bull. Seism. Soc. Am*, 90(6), 1353–1368. https://doi.org/10.1785/012000006

Андрій ГНИП, Дмитро МАЛИЦЬКИЙ

Карпатське відділення Інституту геофізики ім. С. І. Субботіна НАН України, вул. Наукова 3Б, Львів, 79060, e-mail: agnyp.gm@gmail.com, https://orcid.org/0000-0002-2612-4234

## ВИЗНАЧЕННЯ РОЗТАШУВАННЯ ЗЕМЛЕТРУСІВ У КЛАСТЕРАХ І КУТІВ ВИХОДУ ЗА РІЗНИЦЕЮ МІЖ ІНТЕРВАЛАМИ S-P

У статті [Gnyp & Malytskyy, 2023] продемонстровано, як взаємне розташування схожих землетрусів у кластерах можна визначити лише за різницею інтервалів між вступами перших P- і S-хвиль. Перевагою використання лише різниці є те, що, оскільки її визначають з використанням функції взаємної кореляції у вікні довкола відповідних вступів, немає необхідності знати їхній точний час. Інша перевага полягає у тому, що взаємне розташування землетрусів можна визначати незалежно від часу у вогнищі, а отже, від часто неточних вступів і швидкісної моделі. У статті прийнято, що розмір кластера набагато менший за відстань до станцій, і що кути виходу перших P- і S-хвиль й азимути станцій відомі принаймні для одного, опорного землетрусу. Тоді співвідношення між координатами і різницею між інтервалами стає суто геометричним і лінійним, а відповідна система легко розв’язується. Однак, якщо окрім координат, невідомі і кути виходу, система стає нелінійною і настільки сингулярною, що розв’язати її практично неможливо. У цій статті ми пропонуємо обійти сингулярність за допомогою оптимізації координат і кутів виходу окремо: спочатку визначати координати для певних початкових кутів виходу, після того підбирати кути виходу, визначати для них нові координати і т.д. Аби оцінити ефективність такого підходу, виконано серію модельних експериментів, націлених на перевірку можливості повного відновлення координат і кутів виходу з використанням розв’язку загашеного мінімально квадратичного залежно від ступеня неточності початкових кутів, кількості й конфігурації станцій та ступеня загашення розв’язку. Для зменшення впливу локальних мінімумів запропоновано визначати медіану розв'язків, отриманих для ансамблю випадково збурених початкових кутів. Результати тестування свідчать про ефективність запропонованого підходу і доцільність застосування алгоритму до реальних даних. Алгоритм можна застосовувати і в комбінації з іншими методами, пов’язуючи землетруси з нечіткими записами з іншими, параметри яких відомі набагато краще. А це особливо важливо для отримання точнішого уявлення про розломно-блокову тектоніку серединно-континентальних зон зі слабкою сейсмічністю, природу місцевої сейсмічної активності й сейсмічну небезпеку.

*Ключові слова:* розташування землетрусів, кути виходу, визначення координат, схожі землетруси, кластер землетрусів, інтервал між вступами P- та S-хвиль, функція взаємної кореляції.

Received 12.10.2025